Photosynthesis Research **25**: 1–10, 1990.

Regular paper

Fluorescence lifetimes of dimers and higher oligomers of bacteriochlorophyll *c* from *Chlorobium limicola*

Timothy P. Causgrove,[1] Daniel C. Brune,[1] Robert E. Blankenship[1] & John M. Olson[2]
[1]*Department of Chemistry and Center for the Study of Early Events in Photosynthesis, Arizona State University, Tempe, AZ 85287-1604, USA;* [2]*Institute of Biochemistry, Odense University, Campusvej 55, DK 5230 Odense M, Denmark*

Received 8 November 1989; accepted 5 February 1990

Key words: Aggregation, bacteriochlorophyll *c*, *Chlorobium limicola*, chlorosomes, fluorescence, green photosynthetic bacteria

Abstract

Fluorescence lifetimes have been measured for bacteriochlorophyll (BChl) *c* isolated from *Chlorobium limicola* in different states of aggregation in non-polar solvents. Two different homologs of BChl *c* were used, one with an isobutyl group at the 4 position, the other with n-propyl. Species previously identified as dimers (Olson and Pedersen 1990, Photosynth Res, this issue) decayed with lifetimes of 0.64 ns for the isobutyl homolog, 0.71 ns for n-propyl. Decay-associated spectra indicate that the absorption spectrum of the isobutyl dimer is slightly red-shifted from that of the n-propyl dimer. Aggregates absorbing maximally at 710 nm fluoresced with a principal lifetime of 3.1 ns, independent of the homolog used. In CCl_4, only the isobutyl homolog forms a 747-nm absorbing oligomer spectrally similar to BChl *c in vivo*. This oligomer shows non-exponential fluorescence decay with lifetimes of 67 and 19 ps. Because the two components show different excitation spectra, the higher oligomer is probably a mixture of more than one species, both of which absorb at ~747 nm.

Abbreviations: BChl – bacteriochlorophyll; Chl – chlorophyll; χ^2 – chi-square; FWHM – full-width at half-maximum

Introduction

Bacteriochlorophyll (BChl) *c* occurs in chlorosomes of green photosynthetic bacteria in the families Chlorobiaceae (green sulfur bacteria) and Chloroflexaceae (green filamentous bacteria). Chlorosomes are rather flattened, ellipsoidal attenna structures that are unique to the green photosynthetic bacteria. They are approximately 100 nm long, 30 nm wide, and 12 nm thick in *Chlorofexus aurantiacus* and somewhat larger in *Chlorobium* species (Sprague and Varga 1986) and are appressed against the inner surface of the cytoplasmic membrane, which also serves as the photosynthetic membrane (Olson 1980, Blankenship et al. 1988a). Each chlorosome contains about 10 000 molecules of BChl *c* that cooperate in absorbing light and transferring the absorbed energy to the adjacent photosynthetic membrane (van Dorssen et al. 1988, Mimuro et al. 1989, Wang et al. 1990).

The blue and red absorption maxima of BChl *c* in chlorosomes are at 455–460 nm and 740–755 nm, respectively, positions considerably shifted from the 435-nm Soret peak and the 668-nm red peak of BChl *c* extracted into methanol or a similar organic solvent (Brune et al. 1988a, Olson and Pedersen 1990). Furthermore, there is

an increase in extinction coefficient at the red absorption peak accompanied by a decrease in the blue peak of BChl *c* in chlorosomes compared to monomeric BChl *c* in solution. Various lines of evidence indicate that these spectral features are due to direct pigment–pigment interactions between adjacent BChl *c* molecules in chlorosomes. Nearly identical changes in the positions and relative intensities of the BChl *c* absorption maxima occur when BChl *c* aggregates spontaneously in nonpolar solvents (Bystrova et al. 1979, Smith et al. 1983, Olson et al. 1985, Brune et al. 1987). Resonance Raman and infrared spectroscopy reveal similar interactions between BChl *c* molecules in the *in vitro* oligomers and in chlorosomes (Blankenship et al. 1988b, Brune et al. 1988b, Lutz and van Brakel 1988). Finally, circular dichroism measurements on both chlorosomes and *in vitro* BChl *c* oligomers provide evidence for similar strong pigment–pigment interactions in both (Olson et al. 1985, Blankenship et al. 1988b, Brune et al. 1990). Chlorosomes also contain low-molecular weight proteins that may bind to the BChl *c* oligomers and arrange them in an orderly configuration that leads to efficient excitation transfer within the chlorosome antenna (Feick and Fuller 1984, Wechsler et al. 1985, Fetisova et al. 1986, van Dorssen et al. 1986, Gerola et al. 1988, Wagner-Huber et al. 1988).

The distinctive ability of BChl *c* to form aggregates *in vitro* that are similar to those in the chlorosome antenna makes studying the *in vitro* aggregates a convenient way to investigate BChl *c* organization in chlorosomes. In the previous paper in this series, Olson and Pedersen (1990) examined self-association of BChl *c* isolated from *Chlorobium limicola* f. *thiosulfatophilum* in CH_2Cl_2, $CHCl_3$ and CCl_4. They found that the extent of aggregation was controlled by the solvent, the concentration of BChl *c*, and by the BChl *c* homolog used (BChl *c* is a mixture of chemically homologous Mg-chlorin pigments differing slightly in the substituents at positions 4 and 5 on the chlorin ring). Specifically, their experiments showed that BChl *c* containing a n-propyl substitution at the 4-position (PEF–BChl *c*) formed 2 distinct aggregates, designated II_p (which they characterized as a dimer) and III_p, while BChl *c* with an isobutyl substituent at the 4-position (iBM/EF–BChl *c*) formed at least 3 aggregates, designated II_b, III_b and IV_b. They concluded that species II_b is probably a dimer while IV_b, which formed only in CCl_4, is a higher oligomer. It is species IV_b that has spectral properties similar to those of BChl *c* in *Chlorobium* chlorosomes.

Because several aggregated forms of BChl *c* as well as monomeric BChl *c* occurred together in the solvents tested, it was not always easy to determine which absorption bands corresponded to which aggregated BChl *c* species. Olson and Pedersen (1990) approached this problem by deconvoluting the absorption spectra into different Gaussian components. They then assigned these components to particular pigment aggregation states on the basis of changes in their relative amplitudes with increasing pigment concentration (and thus increasing extent of aggregation). They also measured excitation spectra (at wavelengths below 600 nm) for emissions at wavelengths where emission from the different aggregated species was maximal, but for technical reasons, these measurements were not extended above 600 nm. Previous experiments by Brune et al. (1987) showed that 4-ethyl-5-methyl BChl *c* stearyl ester isolated from *Cf. aurantiacus* formed aggregates similar to those observed by Olson and Pedersen (1988, 1990), and that the different aggregated forms had different fluorescence lifetimes. In the experiments reported here, we have measured the fluorescence lifetimes of the different aggregated forms of the BChl *c* homologs from *Cb. limocola* studied by Olson and Pedersen. We have also determined the excitation spectrum for each component identified on the basis of its fluorescence lifetime, as well as the emission spectrum for three of the species. The excitation spectra, which provide a direct measurement of the red absorption spectra of the aggregated species, are compared here with the results from deconvolution into Gaussian curves obtained by Olson and Pedersen (1990).

Materials and methods

The 4-n-propyl and 4-isobutyl homologs of farnesyl BChl *c* were isolated from *Chlorobium limicola* f. *thiosulfatophilum* and purified as described by Olson and Pedersen (1990). The

purified pigments were dried under a stream of N_2 and stored under N_2 at −20°C in vials sealed with teflon-lined rubber septa until used. Anhydrous grades of CH_2Cl_2 and CCl_4 were obtained from Aldrich Chemical Company and stored under N_2 to maintain anhydrous and anaerobic conditions. Heptane (Baker Analysed Reagent) was added to an equal volume of CCl_4 containing dissolved BChl *c* to form the solvent in some experiments.

Samples were prepared immediately before use by injecting the solvent with a 2.5 ml syringe into a septum-sealed vial containing the dried pigment. The dissolved pigment was drawn back into the syringe, which was then attached to a home-built pump. During fluorescence measurements, the sample was pumped through a Hellma quartz flow cell (0.15 cm path length) at 5–10 μl/min to a sealed collecting vial. Pumping was halted between measurements to conserve sample. The pigment concentration was adjusted to give an absorbance between 0.1 and 0.3 at the red absorption maximum of the sample, unless otherwise indicated.

Fluorescence lifetimes of BChl *c* samples were measured by the time-correlated single photon counting method. The frequency-doubled, 532-nm output of a Coherent Antares 76s Nd:YAG laser was routed through a variable beamsplitter to pump either a cavity-damped Spectra-Physics 3500 dye laser operating with DCM as the laser dye or a cavity-dumped Coherent 701-3 dye laser operating with Pyridine 1. The output of the Coherent laser was tunable from 670 nm to 760 nm at 3.8-MHz repetition rate, while DCM was used in the range 650 nm to 700 nm; real-time autocorrelation traces indicated pulse widths of <10 ps. The dye laser output passed through a vertically oriented Glan–Thompson prism polarizer into the flow cell, and emission was collected at a right angle to the excitation through a polarizer oriented at 54.7° from vertical by a Pentax 35 mm camera lens. The emission was then focussed on the entrance slit of a Jobin–Yvon DH-10 double monochromator operated with 0.5-mm slits (4-nm bandpass). The monochromator output impinged on a cooled Hamamatsu R2809-01 S20 response microchannel plate photomultiplier. The resulting photocurrent pulses were amplified by a Phillips 6954B-10 amplifier and fed through a Tennelec TC455 quad constant fraction discriminator (CFD) to the START input of a Tennelec TC864 time-to-amplitude converter (TAC). A fraction of the dye laser output was diverted to a fast photodiode, which triggered a Tennelec TC453 CFD; its output was sent to the STOP input of the TAC. The TAC output was analyzed by pulse height using a Nucleus PCA-II multichannel analyzer, and raw data were then transferred to a Digital Equipment Corp. VAXstation 3200 for deconvolution analysis. Goodness of fit to a sum of exponentials was judged from χ^2 and inspection of weighted residuals. The instrument response function was measured by replacing the sample cuvette with an identical sealed cuvette filled with Ludox AS-40 and adjusting the emission monochromator to the laser wavelength, resulting in a FWHM of about 40 ps. For excitation spectra, the instrument response was measured after each change in laser wavelength. Data files contained 2048 channels each at either 5 or 10 ps/channel (depending on the overall rate of decay), and were collected to 10 000 counts in the peak channel. Laser intensites incident upon the sample varied from 0.01 to 0.4 mW and were generally ~0.05 mW. Absorption spectra of samples were taken at the beginning and end of each day's laser experiments to test for degradation of the pigments or aggregates. All experiments were performed at room temperature.

For each sample, a series of fluorescence decays were collected varying the excitation wavelength with the emission wavelength fixed near the expected fluorescence maximum of the dominant species. The set of decays were then deconvoluted using a global analysis program (Knutson et al. 1983, Holzwarth et al. 1987) in which a series of decays are fit simultaneously to a sum of exponentials. The lifetimes are held independent of wavelength, but the amplitudes are unrestricted, resulting in a set of lifetimes τ_i and amplitudes $A_i(\lambda)$ where i is the number of exponentials. The amplitudes may then be normalized to generate an excitation spectrum for each lifetime component τ_i, or "decay-associated spectrum", as

$$S_i(\lambda) = A_i(\lambda)I(\lambda) \Big/ \sum_i A_i(\lambda)\tau_i$$

where $I(\lambda)$ is the wavelength-dependent emis-

sion intensity (count rate divided by excitation power). The normalized amplitudes $S_i(\lambda)$ are plotted vs. wavelength as a set of curves, each curve corresponding to a decay component τ_i. The normalization procedure is identical for decay-associated emission spectra.

Results

The fluorescence decay was analyzed for five different samples, each promoting the formation of one of the five major species characterized by Olson and Pedersen (1990). We shall report here the results for species II_b, II_p and IV_b; the spectroscopic properties of species III_b and III_p will be discussed in a separate publication. Table 1 lists for each of three samples the homolog used, the solvent, and the approximate BChl *c* concentration. Also listed is the dominant aggregated species; however, absorption spectra (Fig. 1) and their second derivatives (not shown) indicate that each sample contained monomeric BChl *c* as well as a variety of oligomers. Also shown in Fig. 1 is the absorption spectrum of monomeric BChl *c*, which was generated by adding a small amount of methanol to sample #3.

As a consequence of the mixture of species in solution, in nearly all cases the fluorescence decay required a sum of several (3 or 4) exponentials to fit the data. A typical fluorescence decay is shown in Fig. 2, in which sample #2 was excited at 660 nm with fluorescence detected at 706 nm. The data are best fit by a sum of three exponentials with lifetimes of 6.20 ns, 697 ps and 124 ps. The long component may be assigned to the monomer (I_p) on the basis of its known fluorescence lifetime (Brune et al. 1988a). Assignment of other lifetimes to individual species is aided by decay-associated excitation spectra resulting from global analyses. The results of one such analysis performed on sample #1 are depicted in Fig. 3, which plots normalized amplitudes ($S_i(\lambda)$ as described above) vs. excitation wavelength; a sum of five exponentials was used to fit 10 fluorescence decays. The longest component of 6.08 ns is peaked at ~665 nm and is clearly due to the monomer, I_b. The major decay of 660 ps shows a definite peak at 680 nm, and may therefore be assigned to II_b. The 250-ps component shows a peak at ~685 nm and is likely due to III_b. The amplitudes of the 28 ps component show a considerable amount of scatter, but may also peak at 680–690 nm and be associated with III_b. In a four-component analysis, these two shortest lifetimes merge to form a 123-ps component with an increase in overall χ^2 from 1.069 to 1.092. The final component of 1.57 ns shows little or no definite spectrum; components similar to this in lifetime (1–2 ns) and in the lack of defined excitation peaks were observed to a much more pronounced degree in samples which were not flowed. In Fig. 3, this

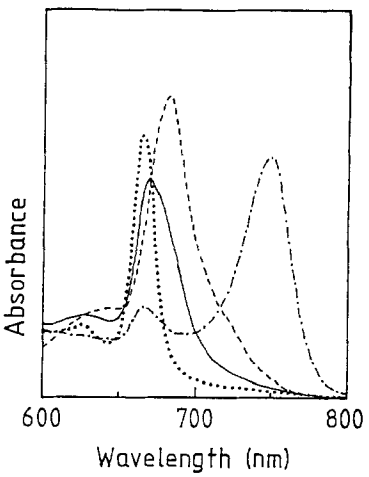

Fig. 1. Red absorption spectra of samples #1 (——), #2 (---) and #3 (– · –) used for fluorescence lifetime experiments and of monomeric BChl *c* (· · ·). The spectra of samples #1, #2 and #3 were recorded in the fluorescence cuvette immediately before lifetime measurements were taken. Peak absorbances of samples used for fluorescence measurements were 0.21 (#1), 0.40 (#2) and 0.15 (#3).

Table 1. Samples used for fluorescence lifetime measurements and dominant aggregated species

Sample	Homolog	Solvent	Conc. (μM)	Species
1	iBM/EF–BChl *c*	CH_2Cl_2	20	II_b
2	PEF–BChl *c*	CH_2Cl_2	30	II_p
3	iBM/EF–BChl *c*	CCl_4/Heptane (50/50)	16	IV_b

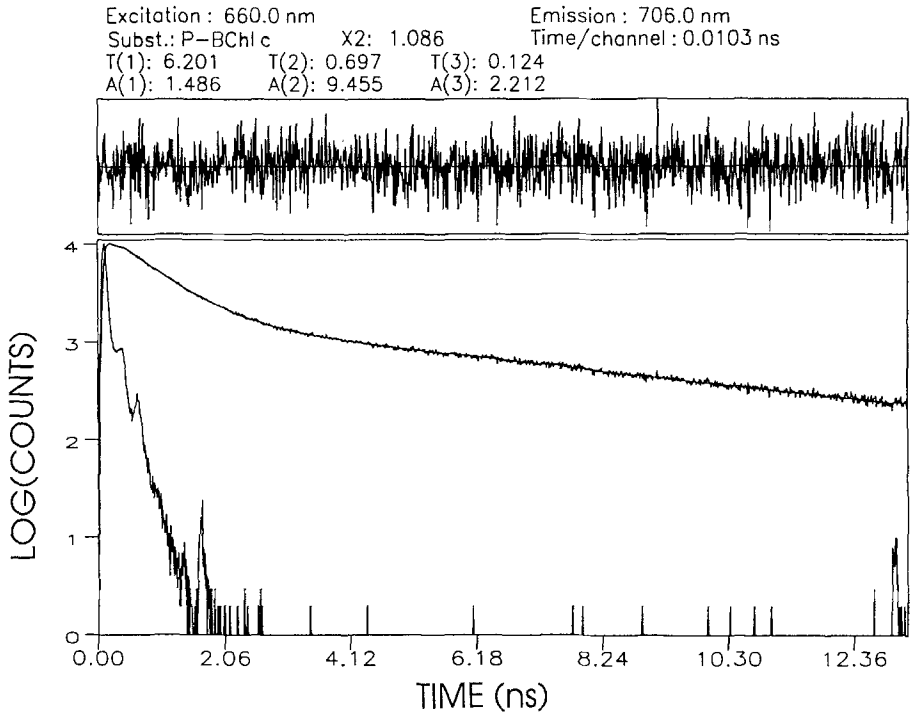

Fig. 2. Fluorescence decay of 30 μM PEF–BChl *c* in CH_2Cl_2 (sample #2) with excitation at 660 nm and emission at 706 nm using 10 ps/channel. Lower data curve is the instrument response function, upper is the fluorescence decay; solid line through the decay is the best fit with a sum of three exponentials. Upper panel is the residuals between data and fitted curves weighted according to the square root of counts in the data channel. Lifetimes are given by T(1) through T(3) in ns and unnormalized amplitudes by A(1) through A(3).

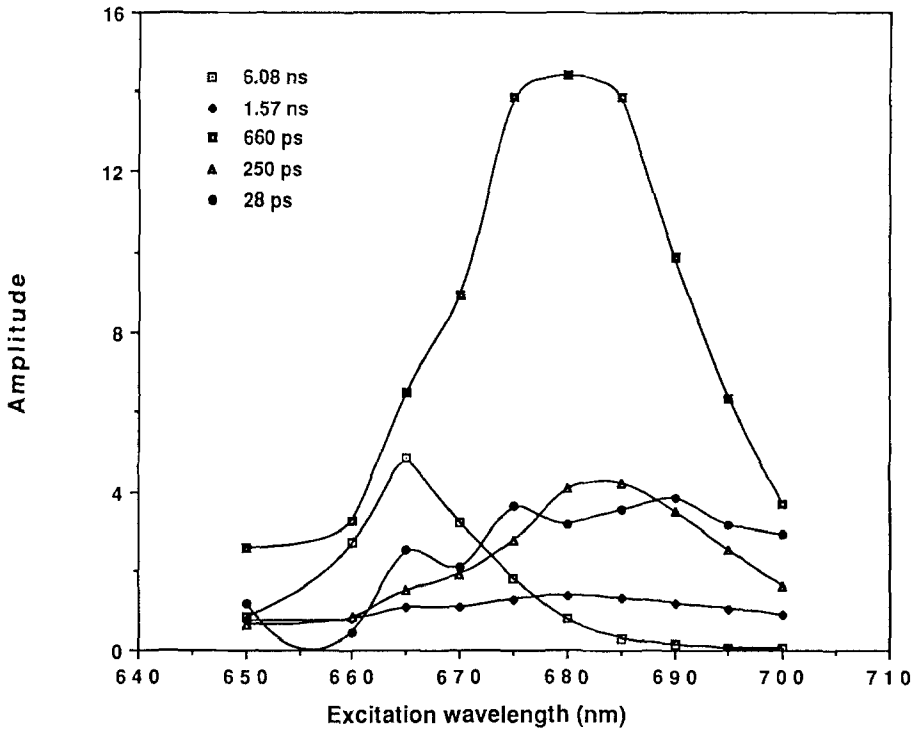

Fig. 3. Decay-associated excitation spectrum of 20 μM iBM/EF–BChl *c* in CH_2Cl_2 (sample #1) using five-component global analysis. Amplitudes were normalized as described in the text; emission wavelength was held fixed at 706 nm.

component reaches a maximum of approximately 10% of the total decay; without the flow system, its amplitude reached 40–50% of the total decay and generally increased with longer laser exposure. It is therefore likely that this intermediate lifetime component is due to BChl *c* breakdown product(s).

A similar experiment was performed on the same sample varying the emission wavelength from 690 nm to 720 nm with the excitation held fixed at 680 nm. The lifetimes resulting from a global analysis of these data are quite consistent with those from the excitation analysis; both sets of results are listed in Table 2. The decay-associated emission spectrum exhibits very little structure for the majority of the components, although II_b emission (637 ps) may show a shoulder at 705 nm (data not shown).

The excitation spectrum of sample #2, PEF–BChl *c* in CH_2Cl_2 (Fig. 4) is in many respects similar to that of Fig. 3, again requiring 5 exponentials; the lifetimes are listed in Table 2. The dimeric species (II_p) shows a maximum at 680 nm, with a lifetime of 713 ps. The contribu-

Table 2. Fluorescence lifetimes (in ns) resulting from global analyses of excitation- and emission-wavelength dependent decays of samples listed in Table 1

Sample	Wavelength scanned	Fixed wavelength	τ_1	τ_2	τ_3	τ_4	τ_5
1	Excitation	706 nm	0.028	0.250	0.660	1.57	6.08
1	Emission	680 nm	0.016	0.253	0.637	1.26	5.79
2	Excitation	706 nm	0.038	0.326	0.713	2.43	6.18
2	Emission	680 nm	0.024	0.375	0.719	2.06	5.83
3	Excitation	765 nm	0.019	0.067	0.379	2.98	–

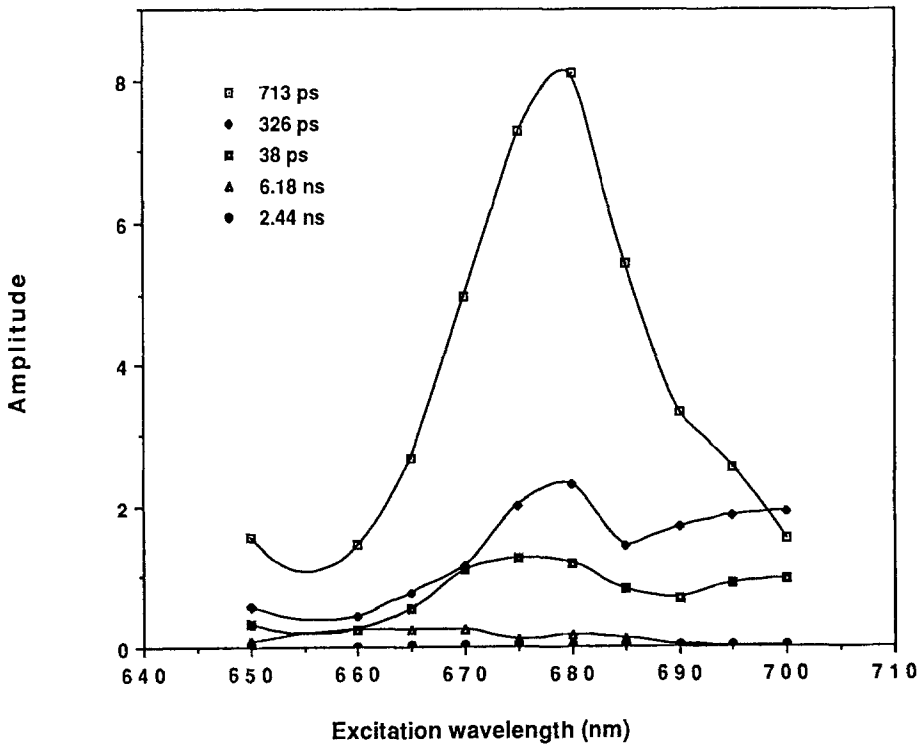

Fig. 4. Decay-associated excitation spectrum of sample #2, also using five-component analysis and 706 nm emission. Amplitudes were normalized as described in the text.

tion of monomer is much smaller in this sample, which is consistent with the observed shift in the absorption maximum from 671 nm in sample #1 to 680 nm in sample #2 as well as a larger dimerization constant for the n-propyl homolog (Olsen and Pedersen 1990). The intermediate lifetime of 2.4 ns is extremely small in amplitude, indicating a greater resistance to the formation of breakdown products in sample #2. As above, two short lifetimes are resolved and are assigned to III_p; fitting the same data with four exponentials increases the overall χ^2 from 1.076 to 1.166. Each of the lifetimes were well-matched in a separate experiment varying the emission wavelength with excitation held at 680 nm (Table 2). The decay-associated emission spectrum again shows little structure although II_p emission appears to peak at ~695 nm with a shoulder at 705 nm.

The fluorescence decay of sample #3 is dominated by very short lifetime components corresponding to the higher oligomer IV_b. Lifetimes resulting from global analysis of 10 fluorescence decay files with excitation from 670 nm to 760 nm are listed in Table 2. The data could also be fit with five exponentials, but the shortest component (8 ps) was near the limit of resolution of the instrument and showed very erratic amplitudes. Therefore, the four-component analysis was judged most appropriate. The decay-associated excitation spectrum from the four-component analysis is shown in Fig. 5; the longest component of 2.98 ns shows a definite peak at 710 nm and is assigned to III_b. The two shortest components, 67 ps and 19 ps, both peaked at ~740–750 nm and are therefore associated with IV_b, with the 67-ps component much broader and more asymmetric. The remaining component of 379 ps is very small in amplitude and shows little wavelength structure, precluding its assignment to a particular BChl *c* species.

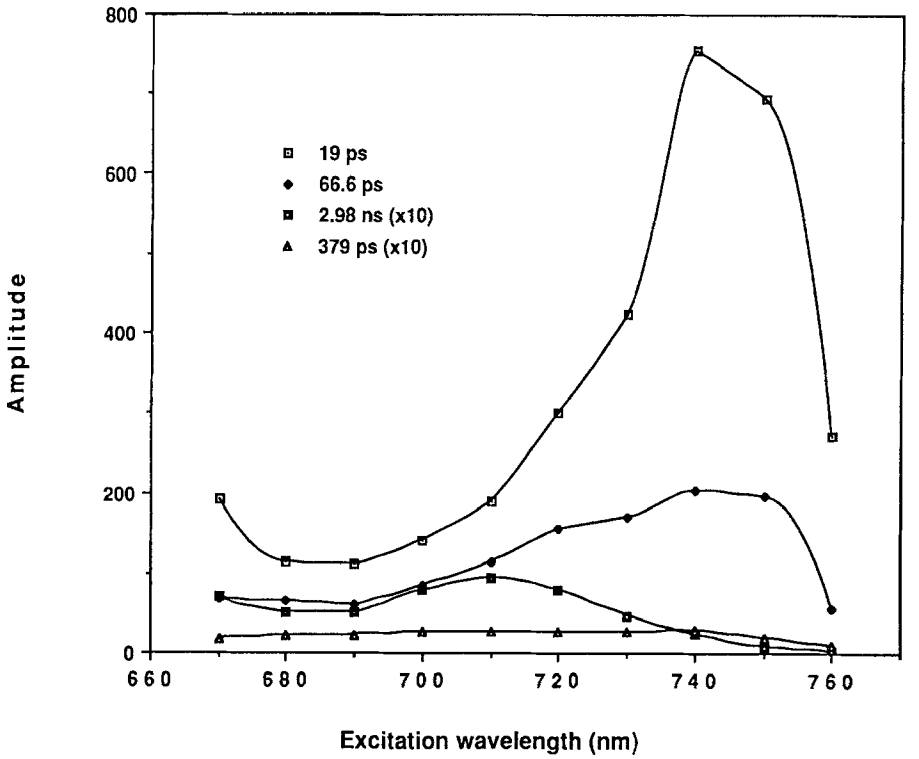

Fig. 5. Decay-associated excitation spectrum of 16 μM iBM/EF-BChl *c* in 50% CCl_4/50% heptane (sample #3) resulting from four-component global analysis; the emission wavelength was 765 nm. The amplitudes were normalized as before, except that the normalized amplitudes of the 2.98 ns and 379 ps components have been multiplied by a factor of 10 to show structure.

Discussion

In the first paper in this series, Olson and Pedersen (1990) examined the absorption and steady-state fluorescence spectra of the n-propyl and isobutyl homologs of BChl *c* in CH_2Cl_2 and CCl_4. In the present work, we have measured the decay-associated excitation spectra of the higher oligomer IV_b and the dimers II_b and II_p. Careful examination of the II_b and II_p excitation peaks in Figs. 3 and 4 (660 ps and 713 ps, respectively) reveals that the II_b excitation peak is broader than that of II_p (27 nm vs. 21 nm FWHM), and that the high-wavelength edge of the II_b spectrum is red-shifted ~5–6 nm from that of the II_p spectrum. The red-shift of II_b from II_p is also evident from the individual spectral points; in the II_b spectrum they are nearly symmetric about the 680 nm point, while for II_p the points are approximately centered about 677–678 nm. Because the FWHM of decay-associated spectra are subject to error due to the low density of points and the dependence on correct normalization at the maximum, the difference in width of II_b and II_p excitation peaks may not be significant.

Comparison of the fluorescence lifetimes of II_b and II_p (Table 2) shows that on the average, fluorescence lifetimes for the species II_b were ~10% higher than those for II_p (716 ps vs. 648 ps, respectively). This difference is larger than standard errors calculated in the global analyses (<10 ps) and larger than the standard deviation in lifetimes resulting from fitting single decays (~35 ps). Because global analysis has been shown to determine lifetimes with higher accuracy than single analyses (Knutson et al. 1983), the difference in lifetime between II_b and II_p appears to be significant, possibly indicating some difference in dimer geometries. It is also noteworthy that the fluorescence lifetimes observed here for BChl *c* dimers are quite different from the lifetime of a Chl *a* dimer, which has been measured as 3.7 ns (Alfano et al. 1985). This Chl *a* dimer has been shown to contain bridging water molecules, while proposed structures of BChl *d* dimers (Smith et al. 1986) are in direct contact via liganding of Mg by a hydroxyethyl group not present in Chl *a*.

The fluorescence lifetime of a higher oligomer of a slightly different homolog of BChl *c* similar to IV_b has already been found to be very short by Brune et al. (1987), who reported lifetimes in the range of 55–135 ps. This compares favorably with the 67 ps lifetime observed here; the fastest component, 19 ps, is below the limit of resolution of the equipment used in those experiments. The fact that both fast components exhibit maxima at ~740–750 nm indicates that the IV_b absorption peak probably results from multiple oligomeric forms. Olson and Pedersen (1990) also suggested that IV_b may represent more than one aggregated species. The data of Fig. 5 suggest that two components with different excitation spectra exist; presumably, the 19-ps component corresponds to a larger oligomer with a greater red shift than the 67-ps component. Species III_p and III_b exhibit fluorescence lifetimes of 30–40 ps, 250–300 ps, and 3 ns; further discussion of this aggregate will be presented elsewhere.

It has been suggested (Mimuro et al. 1989) that oligomers of BChl *c* may be described as J-aggregates, in which the lifetime of an oligomer containing N molecules is τ_m/N_{eff}, where τ_m is the monomer lifetime and N_{eff} is the effective number of molecules in the oligomer ($N_{eff} \leq N$). The Chl *a* dimer lifetime mentioned above, for example, is about half that of the monomer and was explained in terms of a similar aggregate theory. The lifetimes of both dimers of BChl *c* reported here, however, are much shorter than predictions of J-aggregate theory, indicating that quenching is induced upon aggregation. Similar behavior has been observed in dye aggregates, particularly dimers (Lutz et al. 1981, Sundstrom and Gillbro 1985).

The lifetimes of the higher oligomer are difficult to reconcile with those observed in whole cells and intact chlorosomes. Under anaerobic conditions, whole cells of *Cb. vibrioforme* show a lifetime of 68 ps at 760 nm with near 100% energy transfer efficiency to BChl *a* (Blankenship et al. 1990). If the transfer efficiency is taken as 90%, then the intrinsic lifetime of BChl *d* oligomers *in vivo* is calculated as 680 ps, much longer than the observed lifetime of IV_b, clearly indicating that the oligomers are highly quen-

ched. It has been noted that when BChl *a* is removed from isolated chlorosomes, the fluroescence yield from BChl *c* is very low (Griebenow and Holzwarth 1989) and is the same before and after the removal of the baseplate BChl *a* (Brune et al. 1990). This suggests that the procedure to remove BChl *a* induces quenchers which may be similar to those observed here; however, direct comparisons cannot be made because those experiments used chlorosomes from *Chloroflexus*, which has a much different lifetime *in vivo* than *Chlorobium* (Mimuro et al. 1989, Blankenship et al. 1990). Possible decay routes for higher oligomers discussed by Brune et al. (1987) included energy transfer to nonfluorescent impurities in the aggregate chain and an increased rate of internal conversion as compared to the monomer. For the dimer, however, quenching by impurities would not be expected to represent a major decay process. Scherz and Parson (1984) invoked internal conversion to explain the low fluorescence yield of bacteriopheophytin oligomers, and data suggested a metastable state with altered nuclear geometries; a similar mechanism may be operable in the BChl *c* systems. Further experiments, including a temperature-dependent fluorescence study, are required to determine whether this is the correct mechanism for quenching of *in vivo* BChl *c* aggregates.

Acknowledgements

We thank Dr Edith Bittersmann for setting up and testing the fluorescence lifetime apparatus, and Dr Alfred Holzwarth for providing listings of the global analysis software. This is publication #41 from the Arizona State University Center for the Study of Early Events in Photosynthesis. The Center is funded by U.S. Department of Energy grant #DE-FG-88ER13969 as a part of the USDA/DOE/NSF/Plant Science Centers Program. This work was supported by grant #DE-FG-85ER13388 to REB from the Division of Energy Biosciences of the U.S. Department of Energy and grant #DE-FG05-87ER75361 from the DOE University Research Instrumentation Program, and by a grant to JMO from the Danish Natural Science Research Council.

References

Alfano AJ, Lytle FE, Showell MS and Fong FK (1985) Excited singlet-state lifetimes of hydrated chlorophyll aggregates. J Chem Phys 82: 758–764

Blankenship RE, Brune DC and Wittmershaus BP (1988a) Chlorosome antennas in green photosynthetic bacteria. In: Stevens SE, Jr. and Bryant DA (eds) Light-Energy Transduction in Photosynthesis: Higher Plant and Bacterial Models, pp 32–46. Rockville MD: American Society of Plant Physiologists

Blankenship RE, Brune DC, Freeman JM, King GH, McManus JD, Nozawa T, Trost JT and Wittmershaus BP (1988b) Energy trapping and electron transfer in *Chloroflexus aurantiacus*. In: Olson JM, Ormerod JG, Amesz J, Stackebrandt E and Trüper HG (eds) Green Photosynthetic Bacteria, pp 57–68. New York: Plenum Press

Blankenship RE, Wang J, Causgrove TP and Brune DC (1990) Efficiency and kinetics of energy transfer in chlorosome antennas from green photosynthetic bacteria. In: Baltscheffsky M (ed) Proceedings of the VIII International Congress on Photosynthesis. Dordrecht: Kluwer (in press)

Brune DC, Nozawa T and Blankenship RE (1987) Antenna organization in green photosynthetic bacteria. I. Oligomeric bacteriochlorophyll *c* as a model for the 740 nm-absorbing bacteriochlorophyll *c* in *Chloroflexus aurantiacus* chlorosomes. Biochemistry 26: 8644–8652

Brune DC, Blankenship RE and Seely GR (1988a) Fluorescence quantum yields and lifetimes for bacteriochlorophyll *c*. Photochem Photobiol 47: 759–763

Brune DC, King GH and Blankenship RE (1988b) Interactions between bacteriochlorophyll *c* molecules in oligomers and in chlorosomes of green bacteria. In: Scheer H and Schneider S (eds) Photosynthetic Light-Harvesting Systems, pp 141–151. Berlin: Walter de Gruyter

Brune DC, Gerola PD and Olson JM (1990) Circular dichroism of green bacterial chlorosomes. Photosynth Res 24: 253–263

Bystrova MI, Mal'gosheva IN and Krasnovskii AA (1979) Study of molecular mechanism of self-assembly of aggregated forms of bacteriochlorophyll *c*. Mol Biol 13: 582–594

Feick RG and Fuller RC (1984) Topography of the photosynthetic apparatus of *Chloroflexus aurantiacus*. Biochemistry 23: 3693–3700

Fetisova ZG, Karchenko SG and Abdourakhmanov I (1986) Strong orientational ordering of the near-infrared transition moment vectors of light-harvesting antenna bacterioviridin in chromatophores of the green photosynthetic bacterium *Chlorobium limicola*. FEBS Lett 199: 234–236

Gerola PD, Højrup P, Knudsen J, Roepstorff P and Olson JM (1988) The bacteriochlorophyll *c*-binding protein from chlorosomes of *Chlorobium limicola* f. *thiosulfatophilum*. In: Olson JM, Ormerod JG, Amesz J, Stackebrandt E and

Trüper HG (eds) Green Photosynthetic Bacteria, pp 43–52. New York: Plenum Press

Griebenow K and Holzwarth AR (1989) Pigment organization and energy transfer in green bacteria. 1. Isolation of native chlorosomes free of bound bacteriochlorophyll *a* from *Chloroflexus aurantiacus* by gel-electrophoretic filtration. Biochim Biophys Acta 973: 235–240

Holzwarth AR, Wendler J and Suter GW (1987) Studies on chromophore coupling in isolated phycobiliproteins. II. Picosecond energy transfer kinetics and time-resolved fluorescence spectra of c-phycocyanin from *Synechococcus* 6301 as a function of the aggregation state. Biophys J 51: 1–12

Knutson JR, Beechem JM and Brand L (1983) Simultaneous analysis of multiple fluorescence decay curves: a global approach. Chem Phys Lett 102: 501–507

Lutz DR, Nelson KA, Gochanour CR and Fayer MD (1981) Electronic excited state energy transfer, trapping by dimers, and fluorescence quenching in concentrated dye solutions: picosecond transient grating experiments. Chem Phys 58: 325–334

Lutz M and van Brakel G (1988) Ground-state molecular interactions of bacteriochlorophyll *c* in chlorosomes of green bacteria and in model systems. In: Olson JM, Ormerod JG, Amesz J, Stackebrandt E and Trüper HG (eds) Green Photosynthetic Bacteria, pp 23–24. New York: Plenum Press

Mimuro M, Nozawa T, Tamai N, Shimada K, Yamazaki I, Lin S, Knox RS, Wittmershaus BP, Brune DC and Blankenship RE (1989) Excitation energy flow in chlorosome antennas of green photosynthetic bacteria. J Phys Chem 93: 7503–7509

Olson JM (1980) Chlorophyll organization in green photosynthetic bacteria. Biochim Biophys Acta 594: 33–51

Olson JM, Gerola PD, van Brakel GH, Meiburg RF and Vasmel H (1985) Bacteriochlorophyll *a*- and *c*-protein complexes from chlorosomes of green sulfur bacteria compared with bacteriochlorophyll *c* aggregates in CH_2Cl_2-hexane. In: Michel-Beyerle ME (ed) Antennas and Reaction Centers of Photosynthetic Bacteria, pp 67–73. Berlin: Springer-Verlag

Olson JM and Pedersen JP (1988) Bacteriochlorophyll *c* aggregates in carbon tetrachloride as models for chlorophyll organization in green photosynthetic bacteria. In: Scheer H and Schneider S (eds) Photosynthetic Light-Harvesting Systems: Structure and Function, pp 365–373. Berlin: Walter de Gruyter

Olson JM and Pedersen JP (1990) Bacteriochlorophyll *c* monomers, dimers, and higher aggregates in dichloromethane, chloroform, and carbon tetrachloride. Photosynth Res 25: 25–37

Scherz A and Parson WW (1984) Oligomers of bacteriochlorophyll and bacteriopheophytin with spectroscopic properties resembling those found in photosynthetic bacteria. Biochim Biophys Acta 766: 653–665

Smith KM, Kehres LA and Fajer J (1983) Aggregation of bacteriochlorophylls *c*, *d* and *e*. Models for the antenna chlorophylls of green and brown photosynthetic bacteria. J Am Chem Soc 105: 1387–1389

Smith KM, Bobe FW, Goff DA and Abraham RJ (1986) NMR spectra of porphyrins, 28. Detailed solution structure of a bacteriochlorophyllide *d* dimer. J Am Chem Soc 108: 1111–1120

Sprague SG and Varga AR (1986) Membrane architecture of anoxygenic photosynthetic bacteria. In: Staehelin LA and Arntzen CJ (eds) Photosynthesis III, Encyclopedia of Plant Physiology, Vol 19, pp 603–619. Berlin: Springer-Verlag

Sundström V and Gillbro T (1985) Excited state dynamics and photophysics of aggregated dye chromophores in solution. J Chem Phys 83: 2733–2743

Van Dorssen RJ and Amesz J (1988) Pigment organization and energy transfer in the green photosynthetic bacterium *Chloroflexus aurantiacus*. III. Energy transfer in whole cells. Photosynth Res 15: 177–189

Van Dorssen RJ, Vasmel H and Amesz J (1986) Pigment organization and energy transfer in the green photosynthetic bacterium *Chloroflexus aurantiacus*. II. The chlorosome. Photosynth Res 9: 33–45

Wagner-Huber R, Brunisholz R, Frank G and Zuber H (1988) The BChl *c*/*e*-binding polypeptides from chlorosomes of green photosynthetic bacteria. FEBS Lett 239: 8–12

Wang J. Brune DC and Blankenship RE (1990) Effects of oxidants and reductants on the efficiency of excitation transfer in green photosynthetic bacteria. Biochim Biophys Acta 1015: 457–463

Wechsler T, Suter F, Fuller RC and Zuber H (1985) The complete amino acid sequence of the bacteriochlorophyll *c* binding polypeptide from chlorosomes of the green photosynthetic bacterium *Chloroflexus aurantiacus*. FEBS Lett 181: 173–178